ORIGINAL CONTRIBUTION

Rheology measurements of a biomass slurry: an inter-laboratory study

Jonathan J. Stickel · Jeffrey S. Knutsen · Matthew W. Liberatore ·
Wing Luu · Douglas W. Bousfield · Daniel J. Klingenberg · C. Tim Scott ·
Thatcher W. Root · Max R. Ehrhardt · Thomas O. Monz

Abstract The conversion of biomass, specifically ligno-cellulosic biomass, into fuels and chemicals has recently gained national attention as an alternative to the use of fossil fuels. Increasing the concentration of the biomass solids during biochemical conversion has a large potential to reduce production costs. These concentrated biomass slurries have highly viscous, non-Newtonian behavior that poses several technical challenges to the conversion process. A collaborative effort to measure the rheology of a biomass slurry at four separate laboratories has been undertaken. A comprehensive set of rheological properties were measured using several different rheometers, flow geometries, and experimental methods. The tendency for settling, water evaporation, and wall slip required special care when performing the experiments. The rheological properties were measured at different concentrations up to 30% insoluble solids by mass. The slurry was found to be strongly shear-thinning, to be viscoelastic, and to have a significant concentration-dependent yield stress. The elastic modulus was found to be almost an order of magnitude larger than the loss modulus and weakly dependent on frequency. The techniques and results of this work will be useful to characterize other biomass slurries and in the design of biochemical conversion processing steps that operate at high solids concentrations.

Keywords Biomass · Yield stress · Shear thinning · Viscoelasticity · Wall slip

J. J. Stickel (✉)
National Bioenergy Center, National Renewable Energy
Laboratory, Golden, CO 80401, USA
e-mail: jonathan.stickel@nrel.gov

J. S. Knutsen · M. W. Liberatore
Department of Chemical Engineering,
Colorado School of Mines, Golden, CO, USA

W. Luu · D. W. Bousfield
Department of Chemical and Biological Engineering,
University of Maine, Orono, ME, USA

D. J. Klingenberg · T. W. Root · M. R. Ehrhardt · T. O. Monz
Department of Chemical and Biological Engineering
and Rheology Research Center, University of Wisconsin,
Madison, WI, USA

C. T. Scott
U.S. Forest Service Forest Products Laboratory,
Madison, WI, USA

Introduction

Lignocellulosic biomass, i.e., the woody and fibrous parts of plant material, is an abundant natural resource across the globe. Liquid transportation fuels obtained by conversion of the chemical energy stored in lignocellulosic biomass could replace a substantial portion of the petroleum-based fuels consumed world-wide, hence the significant scientific, political, and corporate interest in recent years. Technology currently exists for the biochemical conversion of lignocellulosic biomass to fuel, typically ethanol, but with production costs that are not yet competitive with petroleum-based liquid fuels (Wyman 2007). Several research efforts at the National Renewable Energy Laboratory (NREL) and elsewhere are focused on reducing the cost of biochemical conversion. One possibility for cost-savings is the minimization of added water during the conversion process (Jørgensen et al. 2007; Wingren et al 2003).

Using less water can reduce the size and capital costs of various upstream process vessels, as well as reduce the costs associated with downstream water separation and recycling. Unfortunately, the lower water content, and hence higher solids concentration, can have a negative impact on the process performance when using existing technology and ultimately results in lower conversion yields (Jørgensen et al. 2007). Although the lower process performance at high solids concentrations is due to several factors, including limitations of the commercially available biological catalysts (enzymes and microorganisms), material mixing and mass transfer play a significant role and are clear areas for improvements through application of engineering principles.

Biochemical conversion of lignocellulosic biomass typically occurs in three steps: pretreatment, enzymatic hydrolysis (saccharification), and fermentation (Lynd 1996). The biomass material of interest here is corn stover that has undergone dilute-acid pretreatment (Schell et al. 2003) but has not yet been exposed to enzymes. Corn stover, the stalks, leaves, and cobs of corn plants, is a well-studied feedstock commonly used in lignocellulosic biomass conversion research. Undiluted pretreated corn stover (PCS) ($\sim$ 20% insoluble solids by mass) is a suspension paste: it can easily be formed into a shape that remains when the applied forces are removed (Coussot 2007). In these systems that contain dissolved salts and sugars, as well as cellulose fibers, a distinction needs to be made between total solids and insoluble solids. Total solids includes these dissolved materials and the fibers and particles, while the insoluble solids are only the fibers and particles. The rheology of these systems should mainly depend on the insoluble solids. Performing enzymatic hydrolysis with undiluted PCS poses several challenges, including how to best mix in the enzymes at the beginning of the reaction. An understanding of the rheology of PCS is essential for designing appropriate reaction processes and equipment.

There have been a few studies of the rheology of PCS and other biomass slurries related to biofuels production. Performing rheometry on these materials is quite challenging. As with most yield stress fluids, biomass slurries are prone to wall slip and nonuniform shear profiles (Bertola et al. 2003). The materials are heterogeneous with particles and fibers varying widely in terms of size and aspect ratio. Therefore, reproducible sampling and loading of a rheometer is not trivial. Due to the presence of millimeter-sized particles, jamming is also a problem for narrow-gap geometries. Pimenova and Hanley (2003, 2004) used an impeller device to measure apparent viscosity vs apparent shear rate of PCS at concentrations up to 30%

solids by mass. Yield stress values were determined by fitting to the typical yield stress rheological models of Bingham, Casson, and Herschel-Bulkley (Nguyen and Boger 1992). Dasari and Berson (2007) measured the viscosity of sawdust slurries and Rosgaard et al. (2007) measured the viscosity of barley straw slurries, both using a vane. Their studies were limited to slurries up to 15% solids by mass. Viamajala et al. (2009) used parallel plates to measure viscosity vs shear rate of ground and sieved corn stover, both untreated and pretreated, at concentrations up to 40% *insoluble* solids by mass. Note that the other referenced studies were not clear about the quantity of soluble solids in their samples, such as sugars and salts, that would contribute to a simple measurement of total solids. Yield stress values were determined by fitting to the Casson model. Interestingly, there was a sharp deviation in the yield stress vs concentration trend for concentrations greater than $\sim$ 25% insoluble solids, depending on the sample preparation. This was attributed to the entrainment of air and a shift to granular behavior at these high concentrations, although the possibility of wall slip was not explored. All of these studies were limited to measuring three decades of shear rate or less. More recently, Ehrhardt et al. (2009) and Knutsen and Liberatore (2009) performed rheological studies of PCS simultaneously with the work presented here.

The rheology of wood pulp fiber suspensions, analogous to pretreated biomass slurries, has been well studied for the purposes of paper making. Bennington et al. (1990) used a concentric cylinder device with baffles on both the cylinder and the bob to measure yielding by slowly increasing the applied torque. Damani et al. (1993) performed oscillatory measurements with a reservoir-type parallel plate system with roughened plates. In addition to reporting elastic and viscous moduli as a function of frequency, yield stress values were obtained by measuring the elastic modulus for increasing strain amplitudes. More recently, Ventura et al. (2007) used a Searle-type rotational plate viscometer (Blanco et al. 2007) to measure the shear stress vs shear rate of pulp suspensions. They fit their data to the Herschel-Bulkley model and assessed the effect of pulp properties.

Methods were developed in this work to study the detailed rheological properties of PCS over a concentration range from dilute, flow-able slurries to concentrated, stiff pastes. We performed measurements with a variety of instruments and tools (vanes, roughened plates, and a torque rheometer) in order to produce a comprehensive understanding of the rheology of PCS. By using state-of-the-art rheometers for some of the measurements, oscillatory and uniform shear data were

obtained for much larger ranges of frequency and shear rates than have been previously reported. Comparisons between the different measurement methods help to illustrate which methods are most suited for routine measurements of the rheology of biomass slurries.

Material

The biomass slurry used in this study was corn stover that was chemically pretreated in the Process Development Unit of the National Bioenergy Center at the NREL (Golden, CO). The corn stover, previously ground and sieved with a 5.1-cm (2 in) screen, was treated with dilute sulfuric acid at a loading of 0.048 g/g (acid per dry biomass) and a temperature of 190°C for 1 min (Schell et al. 2003). The total biomass solids concentration during the reaction was 30% by mass. A large portion of the hemicellulose is chemically hydrolyzed by this method, and there is considerable particle size reduction. The particles vary considerably in terms of size (1–2,000 μm; volume-weighted mean ≈ 100 μm) and aspect ratio (1–20), as measured by optical microscopy and image analysis (Particle Size System Research Unit, Clemex Technologies, Longueuil, Québec, Canada). A photograph of undiluted PCS and an optical microscope image of a diluted sample are shown in Fig. 1.

The unmodified PCS is highly acidic (pH ≈ 1.5) and contains soluble sugars that were released by chemical hydrolysis of hemicellulose during the pretreatment. The acidity is enough to etch most stainless steel rheometer tools. In order to raise the pH and remove the dissolved sugars, the PCS is washed with deionized water. The method for washing is to mix in deionized water, centrifuge, decant, and repeat three to six times.

The washed, centrifuged PCS was reconstituted with deionized water to achieve the desired concentrations. All concentrations are reported here as mass percent insoluble solids, as measured by mass ratio upon sample drying. For washed PCS, the amount of insoluble solids equals the amount of total solids. However, it is important to differentiate between insoluble and total solids when comparing to studies with unwashed biomass. Rheological properties should correlate with insoluble solids rather than total solids concentrations. It is difficult to determine the volume fraction of the particles because they are porous and contain a significant portion of the available water in the sample. Estimates based on ongoing work indicate that a concentration of 20% insoluble solids roughly corresponds to a volume fraction of particles of 40% (Roche et al. 2009).

Rheometry

Rheology measurements were made by four different laboratory groups using separate instruments. The instrument used at the NREL was a Bohlin Gemini HR Nano rotational rheometer (Malvern Instruments, Westborough, MA, USA) with a wide-gap vane and parallel plates. The parallel plates were machined to have serrations ∼ 1 mm deep. The instrument used at the Colorado School of Mines (CSM) was an AR-G2 rotational rheometer (TA Instruments, New Castle, DE, USA) with a narrow-gap vane. The instrument used at the University of Maine was a Bohlin CVO rotational rheometer (Malvern Instruments) with parallel plates roughened by the addition of 100-grit sandpaper. A cone and plate geometry was also tested, but the truncated gap was on the order of the particle size and inconsistent results were obtained. The
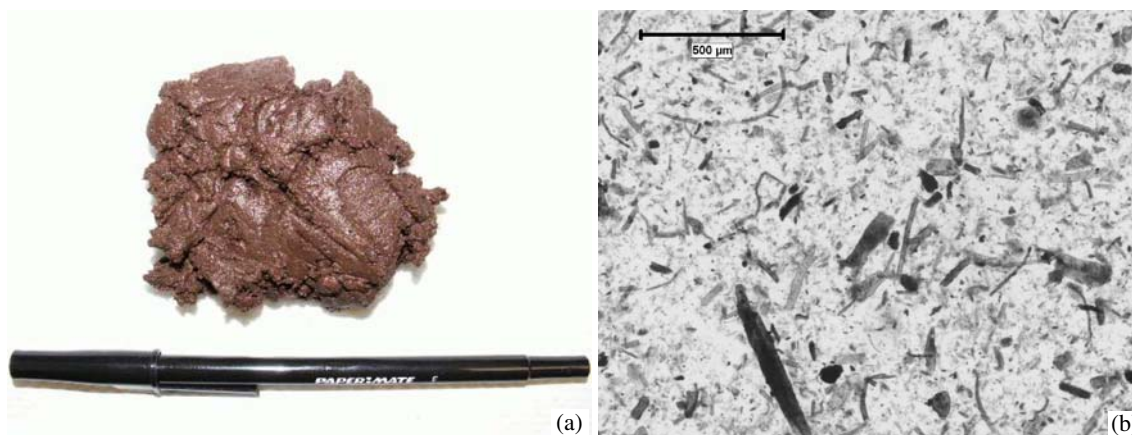

Fig. 1 **a** Photograph of undiluted PCS. **b** Microscope image of PCS particles

Table 1 Instruments and measurement tools used by the different laboratories

Laboratory	Rheometer	Tool(s)
NREL	Bohlin Gemini HR Nano	4-blade vane: $h = 30$ mm, $d = 14$ mm, gap $= 7$ mm
		Parallel plates: $d = 25$ mm, gap ≈ 4 mm
CSM	TA Inst. AR-G2	4-blade vane: $h = 42$ mm, $d = 28$ mm, gap $= 1$ mm
U. Maine	Bohlin CVO	Parallel plates: $d = 40$ mm, gap ≈ 3 mm
U. Wisc. & FPL	Brabender Plasticorder	Impellers: $r_{bowl} = 19.55$ mm, $r_{implr} = 18.7$ mm

instrument used at the University of Wisconsin and US Forest Service Forest Products Laboratory (FPL) was a Plasticorder torque rheometer (Brabender® GmbH, Duisburg, Germany). The instruments and tool dimensions are summarized in Table 1, and photographs of some of the tools are shown in Fig. 2.

Sample handling and loading into the rheometers required special care. Due to settling, washed PCS was well-mixed by hand before taking samples. For the parallel plates, large particles were removed to help prevent jamming. Samples at U. Maine were pushed through a 100-mesh screen (opening $= 150$ μm). Samples at NREL were manually screened with laboratory spatulas to remove particles $\gtrsim 1$ mm. Lowering the top plate onto the samples was also troublesome. Of course, not lowering far enough resulted in poor contact between the plate and the sample. Lowering too far preferentially pressed liquid out of the sample. Reproducible results were obtained by carefully watching (by naked eye) for these two conditions and adjusting the plate height accordingly.

Evaporation of the water was of concern, especially for experiments performed in arid Colorado. Sample containers were always kept tightly closed. Two-piece covers were used around the top of the vanes at both CSM and NREL to reduce evaporation during measurement. For parallel plate measurements, a ring with a 2-mm gap from the plate and a two-piece cover was used at U. Maine. At NREL, a close-fitting collar was used (described below). The torque rheometer is a closed system, and hence, evaporation does not occur. Measurements were performed at a temperature of

25°C, except at U. Maine, where the measurement temperature was 45°C. Temperature in this range seems to have little effect on the measured rheological properties. Enzymatic hydrolysis is typically performed at temperatures between 45°C and 50°C.

For concentrated samples in a parallel plate tool, the sample had a tendency to slide out from between the plates after one to two strain units of deformation. Very little ejection of material needed to occur before there was separation between the sample and the top plate, resulting in erroneous measurements. A collar was used at NREL to prevent the ejection. The collar was cut from a plastic syringe of appropriate diameter so that there was a 0.7-mm gap between the edge of the top plate and the collar (see Fig. 2b). A parallel plate system with side containment was also used by Damani et al. (1993) in their studies of pulp suspensions. Small-angle oscillatory frequency sweeps were performed with the vane and parallel plate tools in the linear region of viscoelastic deformation (strain amplitude $\gamma < 0.001$).

Unidirectional shear flow measurements were performed with parallel plates. At NREL, a decreasing stress ramp, followed by an increasing stress ramp (30 s ramp times for each), was used to measure shear profiles. At U. Maine, quasi-steady measurements were made at discrete stress values, starting at low stress values and increasing to higher values. After an equilibration time, shear rate was averaged over 10 s for each stress. Attempts to measure unidirectional shear flow with the vane tools were not successful: fracture occurred at the edges of the vane, resulting in a slip
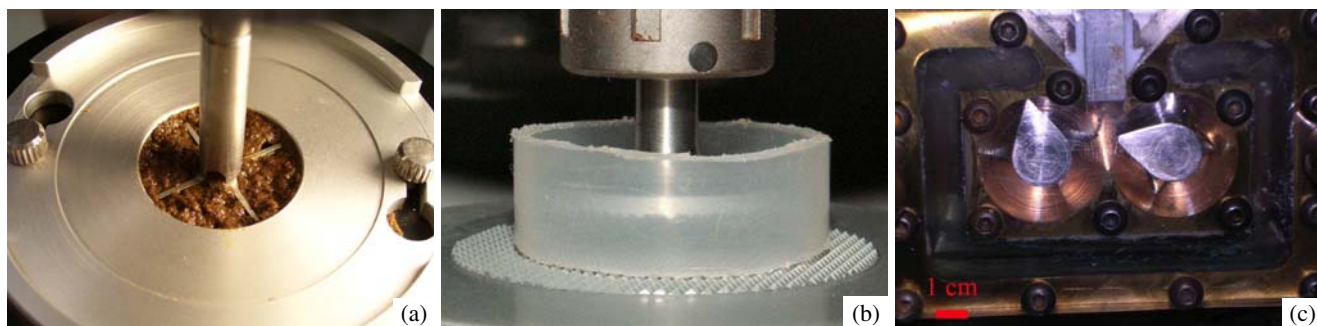
Fig. 2 **a** Narrow gap vane used CSM. **b** Serrated plates and collar used at NREL. **c** Torque rheometer used at U. Wisc

layer between the vane plug and the material in the annulus. Apparent shear stress and shear rate were measured in the torque rheometer at three different speeds. The torque rheometer avoids the problem of material ejection, enabling measurement at higher apparent shear rates. The torque rheometer calibration and experimental methods are described by Ehrhardt (2008).

Although yield stress values can be inferred from shear profile data by extrapolation or model fitting, it is sometimes preferable to determine yield stress values by direct measurement (Nguyen and Boger 1992). One method that was used was rotating a vane at a controlled rate, where the maximum in the torque profile, M_m, was taken to correspond to the dynamic yield stress, τ_y, through the equation (Liddell and Boger 1996):

$$\tau_y = \frac{2}{\pi d^3} \left(\frac{h}{d} + \frac{1}{3} \right)^{-1} M_m, \tag{1}$$

where d and h are the diameter and height of the vane, respectively. A sufficiently low applied rotation rate is necessary to prevent a significant viscous contribution to the measured torque. Yield stress was also measured by oscillatory experiments with increasing amplitude using both the vane and parallel plate tools. The yield stress can be interpreted as the stress amplitude at which the elastic modulus G' becomes smaller than the shear modulus G'', or it can be interpreted as the maximum elastic stress given by $\tau_e = G'\gamma$ (Damani et al. 1993; Shih et al. 1999; Walls et al. 2003; Yang et al. 1986). Analogous to the vane method, a suffi-

ciently low frequency is necessary to prevent significant viscous contributions to the measurement. Although less utilized than other methods to measure yield stress, there are advantages to determining yield stress from dynamic amplitude sweep measurements. Most any rotational rheometry tool can be used, often requiring less sample volume than the vane. By simply including an amplitude sweep with routine rheometry measurements, the yield stress behavior can be probed along with other rheological properties without reloading the sample.

Results and discussion

Results for small-angle oscillatory frequency sweeps are shown in Fig. 3. For these high concentrations, the elastic and viscous moduli increase only slightly over several decades of frequency, with the elastic modulus almost an order of magnitude larger than the viscous modulus. The material is clearly shear thinning, with nearly an order of magnitude drop in complex viscosity for each order of magnitude increase in frequency.

A typical unidirectional shear profile measured by decreasing and increasing stress ramps (NREL, parallel plates with collar) is shown in Fig. 4. The fact that the increasing ramp closely follows the decreasing ramp, especially at the higher shear rates, indicates that there were few issues with sample ejection or sample fracture. However, material would creep out of the gap between the top plate and the collar at shear rates much greater than $100\,\mathrm{s}^{-1}$, limiting the shear rate range that could be
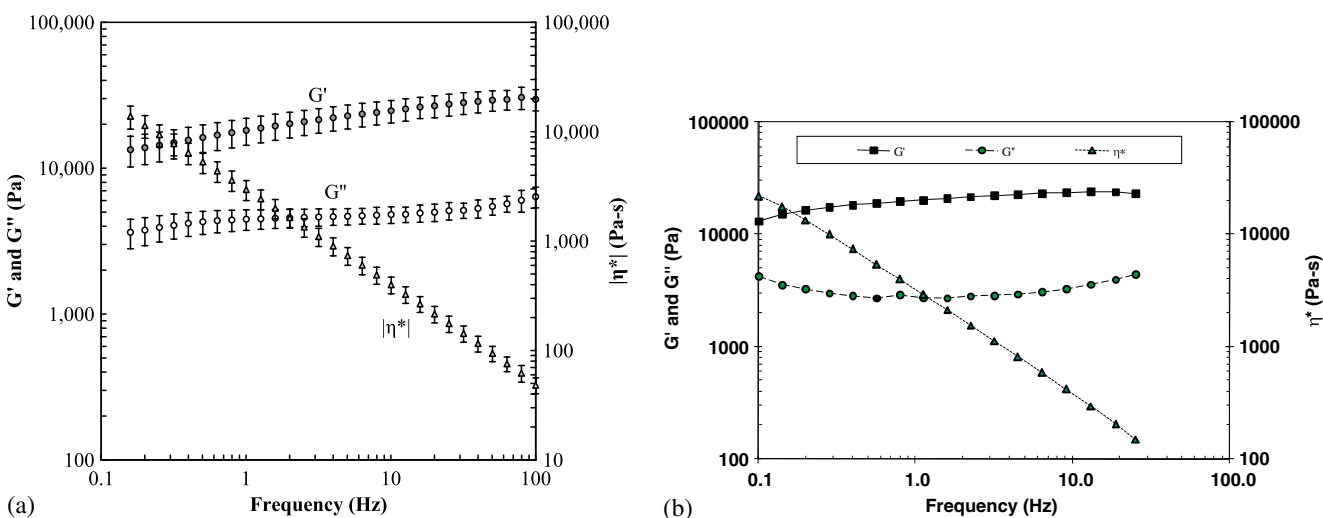

Fig. 3 Elastic and viscous moduli and complex viscosity vs frequency. **a** Measured by the CSM. The concentration was 17% insoluble solids and the applied stress amplitude was 20 Pa.

b Measured by the U. Maine. The concentration was 20% insoluble solids and the applied stress amplitude was 100 Pa
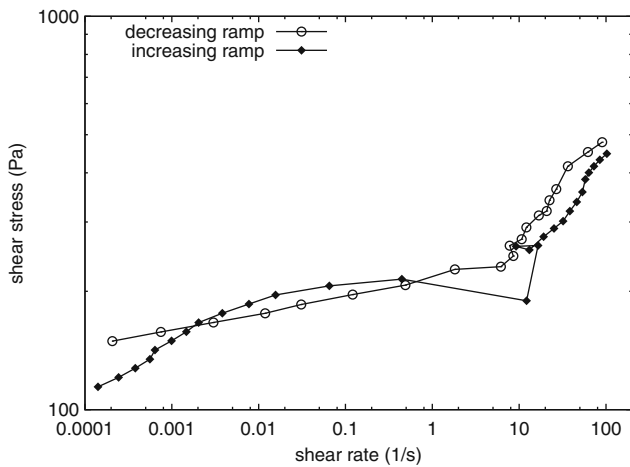
Fig. 4 A typical shear profile result for a decreasing and increasing stress ramp. Measured by NREL at a concentration of 15% insoluble solids

measured with parallel plates. For the increasing ramp, measurable shear rates were obtained at lower applied shear stresses than for the decreasing ramp. This was also observed by Bertola et al. (2003) in model pasty materials where they attribute this creeping behavior at low stresses to unsteady elastic deformation rather than viscous flow. Another notable feature of the increasing ramp is the discontinuity in the slope at the transition from the solid regime to the liquid regime ($\dot{\gamma} \approx 10\,\mathrm{s}^{-1}$ in Fig. 4). We surmise that this arises from a stick-slip phenomenon where the particles momentarily align in the compression direction and then suddenly slide past each other (Stickel et al. 2007). The decreasing ramp seems to mask stick-slip since, initially, the time-scale of the stick-slip events are shorter than the data

acquisition due to the high shear rate; as the shear rate decreases, the particles align and flow essentially stops. Such structural rearrangement is directly related to thixotropy, although we did not study thixotropy in detail in this work. It should be noted that the rearrangement of the microstructure of non-colloidal suspensions (large Peclet numbers) scales with the total strain rather than time (Kolli et al. 2002; Narumi et al. 2002; Voltz et al. 2002). Because the decreasing stress ramp generally avoids the effects of stick-slip and elastic deformation, it provides a better indication of steady shear behavior. The increasing stress ramp data will not be presented further.

Shear profiles for decreasing stress ramps are shown for two concentrations in Fig. 5 along with fits to the Herschel-Bulkley model: $\tau = \tau_y + k\dot{\gamma}^n$ (Nguyen and Boger 1992). Plotting as viscosity vs shear stress in Fig. 5b shows that the material is shear thinning after the initial steep decrease at the yield point.

Since a collar or other containment system was not used by U. Maine, the material slid out from between plates during unidirectional shear flow measurements for shear rates $\dot{\gamma} \gtrsim 1\,\mathrm{s}^{-1}$. Nonetheless, at low shear rates, the measured stress values were reasonably close to those measured at NREL for the same concentrations (results not shown). The tendency of the biomass slurry to eject from parallel plates and fracture at the edge of a vane illustrates how difficult it is to measure the rheology of this material in the liquid regime. Our hypothesis is that, during shear flow, the dominant forces are direct-contact and frictional as the particles collide and slide over one another. These forces combine to push the particles apart, hence the tendency of the sample to expand (plate ejection) or to form particle-depleted regions at a boundary (vane fracture).
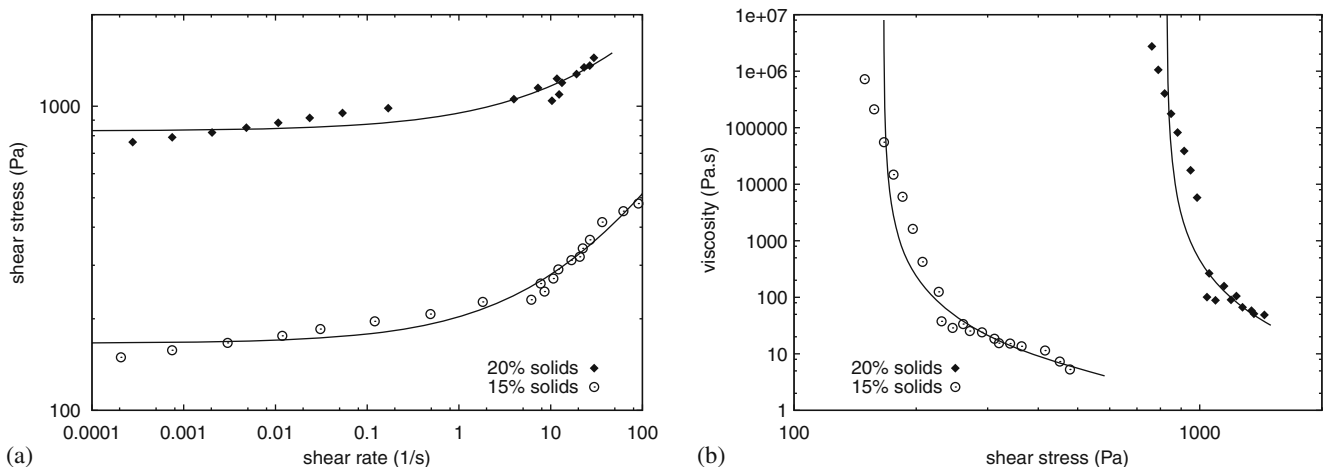

Fig. 5 Decreasing shear stress ramp data measured by NREL along with fits to the Herschel-Bulkley model (**a**, **b**)
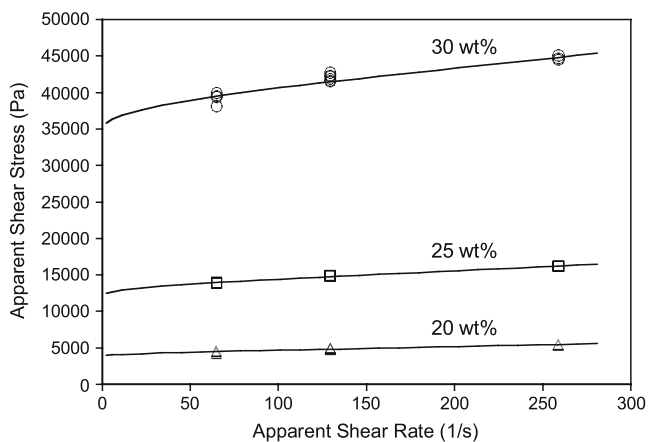
Fig. 6 Apparent shear profiles measured by the torque rheometer (U. Wisconsin and FPL). The *symbols* represent experimental data, and the *curves* represent fits to the Bingham model

These behaviors are likely related to normal stress differences that were not carefully studied in this work, similar to edge fracture in polymer rheometry (Tanner 2000). It is also possible that the shear rate between the parallel plates is nonuniform, perhaps even exhibiting shear-banding (Coussot 2005).

Another way to measure the bulk flow rheology of the material is to use a bulk mixing type device with torque and angular speed measurement on the mixing mechanism. The torque rheometer used by U. Wisc. and FPL employs this concept. The results from the torque rheometer are shown in Fig. 6 along with fitting lines to the Bingham model: $\tau = \tau_y + \eta_p \dot{\gamma}$ (Nguyen and Boger 1992). Due to torque sensitivity limitations, the

lowest concentration that could be measured was 20% insoluble solids. Note that, for a Bingham model fluid, the torque rheometer geometry results in apparent shear stress that is nonlinear in the apparent macroscopic shear rate (Ehrhardt 2008), hence the slight curvature seen in the Bingham model fit lines in Fig. 6. Again, the shear may not be uniform in the bowl, but the apparent shear stress and shear rate profiles provide considerable information about the bulk flow behavior of the material.

Example results from yield stress measurements using the vane tools are shown in Fig. 7. A clear peak is observed that varies little with the applied constant rotation rate for the slow rates that were used. The torque decreases with rotation after passing through the maximum, again illustrating the thixotropy of these materials. Example results from yield stress measurements using oscillatory amplitude sweeps are shown in Figs. 8 and 9. Sample was reloaded for each of the repeat experiments shown in Fig. 8, illustrating the repeatability of the measurements.

The different measures of yield stress result in different values, with the following order: constant rotation rate vane method > moduli crossover method > maximum elastic stress method. The vane method, where the yield point corresponds to the maximum measured torque, gives the dynamic yield stress, i.e., the stress that results in continuously deforming flow (Liddell and Boger 1996; Nguyen et al. 2006). The maximum elastic stress from oscillatory amplitude sweep measurements instead corresponds to the static yield point, i.e., where there is the first deviation from linear elastic
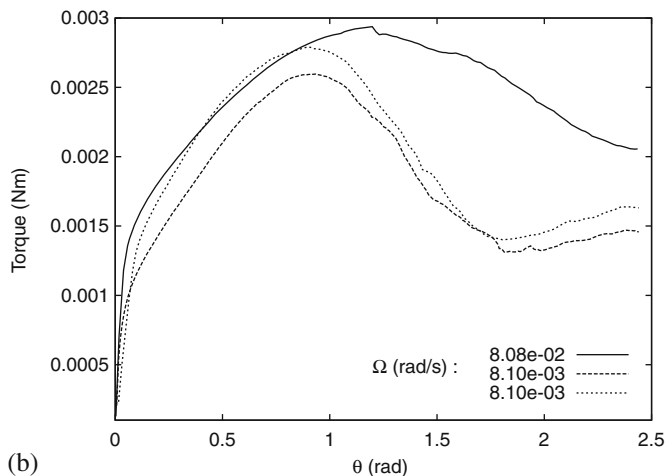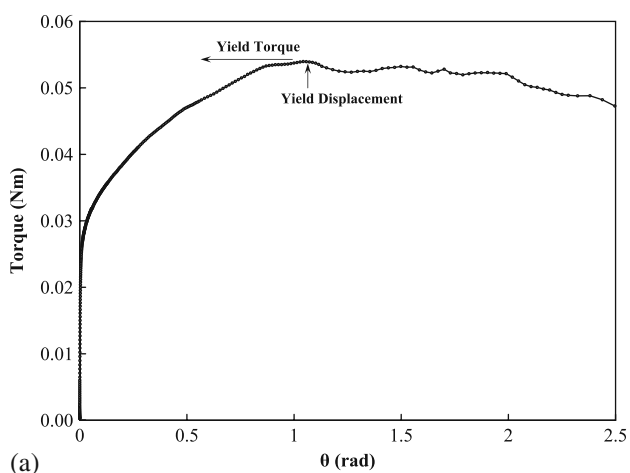

(a)

(b)

Fig. 7 Yield stress measurements by constant rotation rate of a vane. The yield stress is calculated from the maximum torque using Eq. 1. **a** Measured by CSM at a concentration of 17% insoluble solids. The applied rotation rate was 0.007 rad/s, and the calculated yield stress was 896 Pa. **b** Measured by NREL. The *legend* indicates the applied rotation rate for each measurement. The concentration was 15.4% insoluble solids, and the average yield stress calculated from the three measurements was 260 Pa
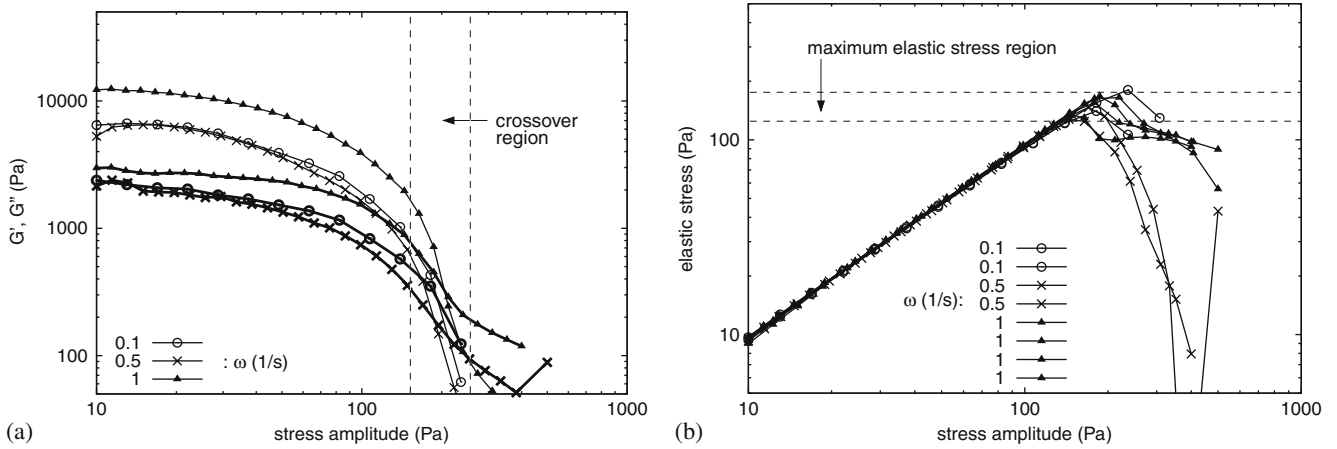
Fig. 8 Oscillatory amplitude sweep results measured by NREL with parallel plates at a concentration of 15.4% insoluble solids. The *legend* indicates the frequency used for each measurement shown. **a** Elastic (*thin lines*) and viscous (*thick lines*) moduli vs stress amplitude. The average for the crossover yield stress values from eight repeat measurements was 204 Pa. Note: some of the repeat measurements are not shown for visual clarity. **b** Elastic stress vs stress amplitude. The average value for the maximum elastic stress (yield stress) for eight repeat measurements was 152 Pa

deformation. This is observed very clearly in the plots of elastic stress vs stress amplitude, where the elastic stress is almost directly proportional to the stress amplitude before the yield point. At the yield point, the measured elastic stress deviates sharply from this linear trend and reaches a maximum as the applied stress is taken up by viscous flow. The crossover method provides yield values that are somewhere in between the static and dynamic yield points with a less clear physical interpretation (Shih et al. 1999; Walls et al. 2003). The crossover, i.e., where $G' = G''$, occurs at deformations where the viscoelastic behavior is nonlinear, and hence, G' and G'' describe only part of the deformation behav-

ior. Although progress might be made by using a more advanced a mathematical treatment of the nonlinear viscoelasticity (Ewoldt et al. 2008; Yao et al. 2008), it is straightforward to use the maximum elastic stress method with the same set of experimentally obtained data.

Yield stress values from all four of the laboratories are plotted against insoluble solids concentration in Fig. 10. The agreement between the data sets is surprisingly good. Yield stress measured by the unidirectional vane method is consistently higher than from the elastic stress method, as discussed above. There is generally an order of magnitude increase in the yield stress for
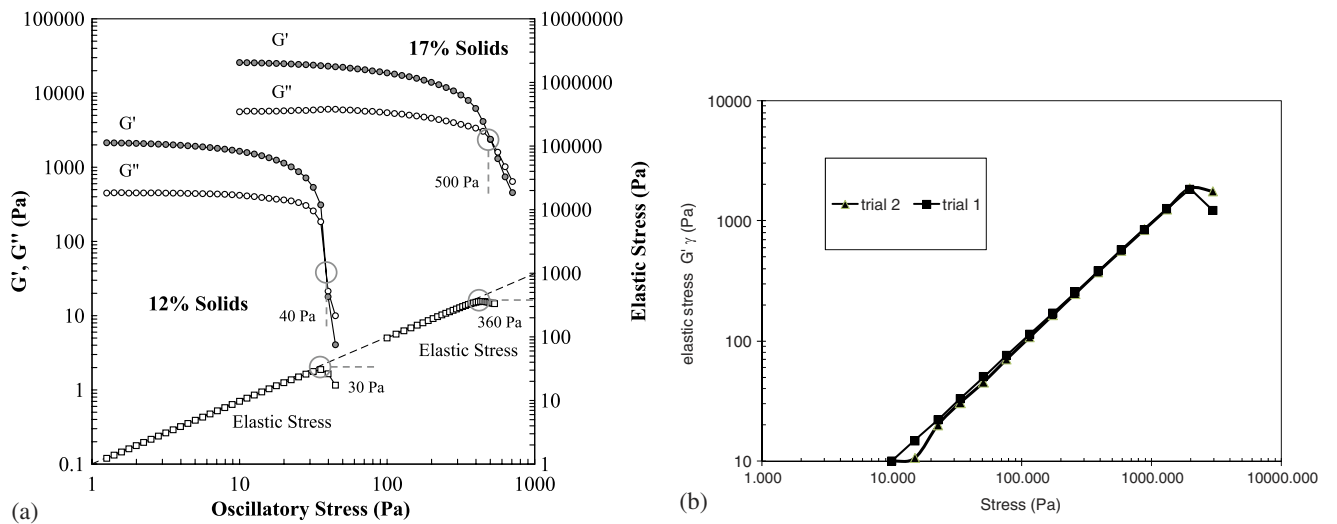

Fig. 9 Oscillatory amplitude sweep results. **a** Measured by CSM with a vane. **b** Measured by U. Maine with rough parallel plates. The concentration was 20% insoluble solids. The maximum elastic stress (yield stress) was 2,000 Pa
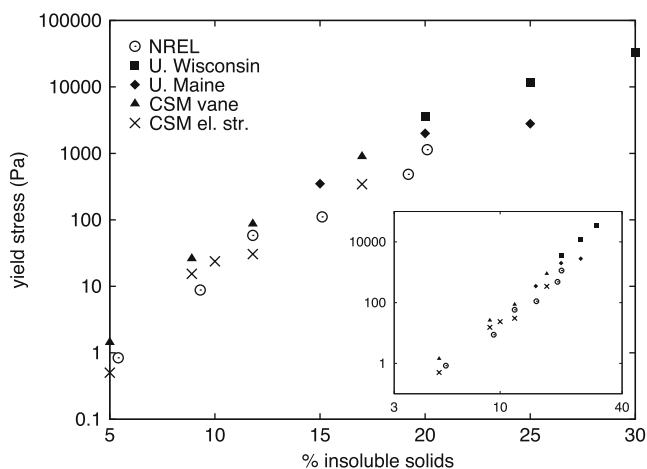
Fig. 10 Yield stress vs insoluble solids concentration. NREL and U. Maine used the elastic stress method with parallel plates. The two data sets from CSM are from the unidirectional vane method and from the elastic stress method (also using the vane tool). U. Wisconsin values are from fitting to the Bingham model. The *inset* shows the same data with logarithmic scaling for both axes

every 5% increase in the insoluble solids concentration. The data are replotted in a log–log plot in the inset of Fig. 10, which reveals a power-law dependence between the yield stress τ_y and the mass concentration C_m: $\tau_y = aC_m^b$. Fitting the power-law to the data gives $b = 5.7 \pm 0.5$. Such power-law behavior is commonly observed in natural and synthetic fiber systems, where the value of the exponent b varies from one system to another. For other acid-hydrolyzed corn stover systems, data reported by Pimenova and Hanley (2004) for total solids concentrations in the range of 5–15 wt.% yield an exponent of 4.6, and Knutsen and Liberatore (2009) reported an exponent of 6 for a concentration range of 5–30 wt.%. Ehrhardt et al. (2009) reported an exponent of approximately 4 for hammermilled stover hydrolyzed at various temperatures, over the range of concentrations 20–35 wt.%. The slightly larger exponent obtained in the present study and by Knutsen and Liberatore (2009) may be related to the larger range of concentrations employed. Power-law exponents reported for wood fiber systems are typically smaller, ranging from 2–4 (Bennington et al. 1990; Dalpke and Kerekes 2005; Kerekes 2006; Swerin et al. 1992). A power-law dependence of the yield stress on fiber concentration has also been observed in simulations of suspensions of flexible fibers that interact via short-range repulsive and friction forces (Switzer and Klingenberg 2003); an exponent of $b = 2.75 \pm 0.80$ was reported. For wood fiber systems and well-defined systems used in simulations, the smaller values for the power law exponent may be related to more uniform morphology and length distributions.

It is clear that yield stress is the rheological property of primary consideration for concentrated PCS slurries. Fortunately, the yield stress can be reliably measured by a variety of instruments and methods, as illustrated by the agreement of the data in Fig. 10. We found that performing an amplitude sweep to determine the maximum elastic stress was a particularly effective method for measuring the yield stress. This can be performed with most modern rotational rheometers and with either a vane or parallel plate geometry. Parallel plates provide the advantage that a relatively small sample size can be used, although the plates should have roughened surfaces to prevent slip, and a large gap may be needed to reduce the possibility of jamming. A torque rheometer enables measurements at higher concentrations. A summary of the capabilities of the different instruments for measuring the rheology of biomass slurries is given in Table 2.

The yield stress will impose the minimum power requirements for pumps, mixers, and other process equipment needed for moving biomass slurries. For example, if the biomass slurry settles out and embeds a mixer, the mixer must have enough power to overcome the yield stress for any motion to occur. Another complication that can arise in a vertical mixing vessel due to yield behavior is buildup of material around the edges of the vessel that does not experience mixing. Therefore, for concentrated biomass slurries undergoing reaction, it is likely that traditional stirred-tank reactors will not be adequate. Novel reactor geometries and mixing mechanisms are being developed for this reason (Jørgensen et al. 2007). The strong correlation between yield stress and concentration should be noted: if working with a concentrated biomass slurry, perhaps a small amount of dilution could reduce yield stress to a reasonable order

Table 2 Capabilities of the instruments for measuring the rheology of biomass slurries

	Parallel plate	Vane	Torque rheometer
Sample volume (ml)	1–5	~35	100
Conc. (wt.% insol. solids)	0–20	0–20	20–40
Shear rate range (1/s)	10^{-3}–10^2	10^{-3}–10^{2a}	50–300
Oscillatory measurement	Yes	Yes	No
Yield stress method	[b,c]	[c,d]	[b]
Considerations	Jamming, ejection, slip	Fracture[a]	Inhomogeneous shear field

[a]Fracture occurs with the vane for slurry concentrations >10 wt.%
[b]Yield stress determined by extrapolation from shear profile data
[c]Yield stress determined by oscillatory amplitude sweep
[d]Yield stress determined from torque maximum during slow rotation

of magnitude for standard liquid handling equipment. At ∼ 20% insoluble solids, the yield stress is on the order of 1,000 Pa. However, the PCS is "pourable" at a concentration of ∼ 10% insoluble solids, which corresponds to a yield stress of ∼ 10 Pa. For practical purposes, the yield stress is effectively zero for concentrations below 5% insoluble solids. The yield stress of PCS also drops dramatically during further saccharification, typically by enzyme catalyst, as the cellulose solids are broken into soluble species (Roche et al. 2009).

Probing the unidirectional shear rheology of PCS proved to be difficult due to non-uniform shear, stick-slip events, and ejection of material, as described above. Further measurements employing other techniques, e.g., capillary rheometry, may be helpful to gain a better understanding of the shear flow behavior of PCS slurries. Extensional flow rheology, e.g., squeeze flow between parallel plates, would also be useful, although Knutsen and Liberatore (2009) report a tendency of the liquid phase to preferentially flow out of the particulate phase during squeeze flow experiments. Despite these challenges, it is clear that the material shears easily for imposed shear stresses above the yield stress: for less than an order of magnitude increase in the shear stress, the shear rate increases by several orders of magnitude (Fig. 5a) and, hence, the viscosity decreases by several orders of magnitude (Fig. 5b). This means that, once the yield stress is overcome, very little additional energy is needed to impose a bulk flow. Additionally, some of the phenomena that make rheology measurements difficult could possibly be helpful. For example, transport in pipes will be aided by wall slip, and fracture can be helpful in transport by gravity feeding or conveying and in mixing by rotary tumbling.

Conclusions

A comprehensive set of rheological properties was measured for PCS, with a variety of instruments and rheometry methods. There was generally good agreement in the results from the different groups and methods, especially for measurements of yield stress, which dominates the rheological behavior of the PCS. Roughened parallel plates were shown to be well suited for measuring nearly all of the rheological properties studied. With a single sample loaded between the plates, dynamic moduli, the static yield stress, and a shear profile were all determined by sequential oscillatory and unidirectional shear experiments. Side containment in the form of a collar was needed to prevent material ejection during the shear experiments. A torque rheometer enabled shear measurements at higher con-

centrations of insoluble solids and at higher shear rates than could be measured in the parallel plates. A vane geometry was shown to be useful for measuring the dynamic yield stress. However, unless high shear rate or dynamic (rather than static) yield information is needed, roughened parallel plates are sufficient for measuring the rheology of PCS.

Undiluted PCS with a concentration of 20% insoluble solids was found to have the rheological properties of a thick, stiff paste. At this concentration, the elastic modulus was measured to be almost an order of magnitude larger than the viscous modulus, and yield stress values were measured on the order of 1,000 Pa. The PCS is shear thinning for applied shear stresses above the yield point.

The measured rheological properties of PCS, and the developed rheometry methods, will be useful in lignocellulosic biochemical conversion research and development. The high yield stress and shear thinning behavior of the concentrated pretreated biomass indicate that traditional tanks stirred with impellers are not adequate as reaction vessels for enzymatic hydrolysis of the biomass, at least not for the start of the reaction. The rheometry methods will be useful for studying the rheology of other types of lignocellulosic biomass, biomass pretreated with different pretreatment conditions, and the biomass slurry as the enzymatic hydrolysis reaction progresses. These research efforts will help enable cost-effective biochemical conversion of lignocellulosic biomass to biofuels.

References

Bennington CPJ, Kerekes RJ, Grace JR (1990) The yield stress of fiber suspensions. Can J Chem Eng 68(5):748–757

Bertola V, Bertrand F, Tabuteau H, Bonn D, Coussot P (2003) Wall slip and yielding in pasty materials. J Rheol 47(5):1211–1226

Blanco A, Negro C, Fuente E, Tijero J (2007) Rotor selection for a searle-type device to study the rheology of paper pulp suspensions. Chem Eng Process 46(1):37–44

Coussot P (2005) Rheometry of pastes, suspensions, and granular materials: applications in industry and environment. Wiley, Hoboken

Coussot P (2007) Rheophysics of pastes: a review of microscopic modelling approaches. Soft Matter 3(5):528–540

Dalpke B, Kerekes RJ (2005) The influence of fibre properties on the apparent yield stress of flocculated pulp suspensions. J Pulp Pap Sci 31(1):39–43

Damani R, Powell RL, Hagen N (1993) Viscoelastic characterization of medium consistency pulp suspensions. Can J Chem Eng 71(5):676–684

Dasari RK, Berson RE (2007) The effect of particle size on hydrolysis reaction rates and rheological properties in cellulosic slurries. Appl Biochem Biotechnol 137:289–299

Ehrhardt MR (2008) Rheology of biomass. Master's thesis, University of Wisconsin, Madison, WI

Ehrhardt MR, Monz TO, Root TW, Connelly RK, Scott CT, Klingenberg DJ (2009) Rheology of dilute acid hydrolyzed corn stover at high solids concentration. Appl Biochem Biotechnol. doi:10.1007/s12010-009-8606-z

Ewoldt RH, Hosoi AE, McKinley GH (2008) New measures for characterizing nonlinear viscoelasticity in large amplitude oscillatory shear. J Rheol 52(6):1427–1458

Jørgensen H, Vibe-Pedersen J, Larsen J, Felby C (2007) Liquefaction of lignocellulose at high-solids concentrations. Biotechnol Bioeng 96(5):862–870

Kerekes RJ (2006) Rheology of suspensions—rheology of fibre suspensions in papermaking: an overview of recent research. Nord Pulp Paper Res 21(5):598–612

Knutsen JS, Liberatore MW (2009) Rheology of high-solids biomass slurries for biorefinery applications. J Rheol 53: 877–892

Kolli VG, Pollauf EJ, Gadala-Maria F (2002) Transient normal stress response in a concentrated suspension of spherical particles. J Rheol 46(1):321–334

Liddell PV, Boger DV (1996) Yield stress measurements with the vane. J Non-Newton Fluid Mech 63(2–3):235–261

Lynd LR (1996) Overview and evaluation of fuel ethanol from cellulosic biomass: technology, economics, the environment, and policy. Annu Rev Energy Environ 21:403–465

Narumi T, See H, Honma Y, Hasegawa T, Takahashi T, Phan-Thien N (2002) Transient response of concentrated suspensions after shear reversal. J Rheol 46(1):295–305

Nguyen QD, Boger DV (1992) Measuring the flow properties of yield stress fluids. Annu Rev Fluid Mech 24:47–88

Nguyen QD, Akroyd T, De Kee DC, Zhu LX (2006) Yield stress measurements in suspensions: an inter-laboratory study. Korea-Aust Rheol J 18(1):15–24

Pimenova NV, Hanley TR (2003) Measurement of rheological properties of corn stover suspensions. Appl Biochem Biotechnol 106:383–392

Pimenova NV, Hanley AR (2004) Effect of corn stover concentration on rheological characteristics. Appl Biochem Biotechnol 114:347–360

Roche CM, Dibble CJ, Knutsen JS, Stickel JJ, Liberatore MW (2009) Particle concentration and yield stress of biomass slurries during enzymatic hydrolysis at high-solids loadings. Biotechnol Bioeng 104(2):290–300

Rosgaard L, Andric P, Dam-Johansen K, Pedersen S, Meyer AS (2007) Effects of substrate loading on enzymatic hydrolysis and viscosity of pretreated barley straw. Appl Biochem Biotechnol 143(1):27–40

Schell DJ, Farmer J, Newman M, McMillan JD (2003) Dilute-sulfuric acid pretreatment of corn stover in pilot-scale reactor—investigation of yields, kinetics, and enzymatic digestibilities of solids. Appl Biochem Biotechnol 105:69–85

Shih WY, Shih WH, Aksay IA (1999) Elastic and yield behavior of strongly flocculated colloids. J Am Ceram Soc 82(3):616–624

Stickel JJ, Phillips RJ, Powell RL (2007) Application of a constitutive model for particulate suspensions: Time-dependent viscometric flows. J Rheol 51(6):1271–1302

Swerin A, Powell RL, Oedberg L (1992) Linear and nonlinear dynamic viscoelasticity of pulp fiber suspensions. Nord Pulp Paper Res 7(3):126–143

Switzer LH, Klingenberg DJ (2003) Rheology of sheared flexible fiber suspensions via fiber-level simulations. J Rheol 47(3):759–778

Tanner RI (2000) Engineering rheology, 2nd edn. Oxford University Press, Oxford

Ventura C, Blanco A, Negro C, Ferreira P, Garcia F, Rasteiro M (2007) Modeling pulp fiber suspension rheology. TAPPI J 6(7):17–23

Viamajala S, McMillan JD, Schell DJ, Elander RT (2009) Rheology of corn stover slurries at high solids concentrations—effects of saccharification and particle size. Bioresour Technol 100(2):925–934

Voltz C, Nitschke M, Heymann L, Rehberg I (2002) Thixotropy in macroscopic suspensions of spheres. Phys Rev E 65(5):051402-1–051402-5

Walls HJ, Caines SB, Sanchez AM, Khan SA (2003) Yield stress and wall slip phenomena in colloidal silica gels. J Rheol 47(4):847–868

Wingren A, Galbe M, Zacchi G (2003) Techno-economic evaluation of producing ethanol from softwood: Comparison of ssf and shf and identification of bottlenecks. Biotechnol Prog 19(4):1109–1117

Wyman CE (2007) What is (and is not) vital to advancing cellulosic ethanol. Trends Biotechnol 25(4):153–157

Yang MC, Scriven LE, Macosko CW (1986) Some rheological measurements on magnetic iron-oxide suspensions in silicone oil. J Rheol 30(5):1015–1029

Yao NY, Larsen RJ, Weitz DA (2008) Probing nonlinear rheology with inertio-elastic oscillations. J Rheol 52(4):1013–1025